Journal of Molecular Liquids 320 (2020) 114415

Contents lists available at ScienceDirect

Journal of Molecular Liquids

journal homepage: www.elsevier.com/locate/molliq

A theoretical study of the magnetic shielding of ^{15}N of formamide in liquid water

Rodrigo Gester [a], Marcus V.A. Damasceno [b], Sylvio Canuto [c], Vinícius Manzoni [d,*]

[a] Faculdade de Física, Universidade Federal do Sul e Sudeste do Pará, 68507-590 Marabá, PA, Brazil
[b] Faculdade de Ciências Biológicas, Agrárias, Engenharia e da Saúde, Universidade do Estado de Mato Grosso (UNEMAT), 78300-000 Tangará da Serra, MT, Brazil
[c] Instituto de Física, Universidade de São Paulo, Rua do Matão 1371, 05508-090 São Paulo, SP, Brazil
[d] Instituto de Física, Universidade Federal de Alagoas, 57072-970 Maceió, AL, Brazil

ARTICLE INFO

Article history:
Received 17 July 2020
Received in revised form 11 September 2020
Accepted 22 September 2020
Available online 28 September 2020

Keywords:
NMR shielding
Formamide
Solvent effect
Molecular modelling
s-MC/QM methodology

ABSTRACT

The solvent effect on ^{15}N magnetic shielding constants of hydrated formamide was studied using the sequential Monte Carlo/Quantum Mechanics (s-MC/QM) methodology. For this, a detailed analysis was made using several solvent models that include the use of explicit and implicit molecules. The most accurate description of the magnetic shielding constant was performed using the solvent model including the solute-solvent hydrogen-bonded structures embedded in the electrostatic field of the remaining bulk solvent molecules. This description gives a downfield effect of -38.5 ± 0.8 ppm on ^{15}N magnetic shielding of hydrated formamide. Moreover, the downfield effect was also observed in all models of solvent considered. However, the use of the partial description of the solvent using the continuum model or considering only the inclusion of the close neighboring molecules or only the electrostatic embedding of the solvent are not able to give the total paramagnetic contribution for the magnetic shielding. In fact an incomplete description is also obtained if only considering the inclusion of the close neighboring molecules. The direct comparison with some other solvated nitrogen based systems such azines and ammonia indicates that the protic nature of formamide nitrogen is the main responsible for the large downfield in the signal of the gas-solvent $\Delta\sigma(^{15}N)$ NMR shift.

1. Introduction

Nuclear magnetic resonance (NMR) is used for obtaining information about both the molecular structure and the chemical environment [1,2]. For these reasons, since it was first discovered in 1960, NMR has emerged as a powerful tool for molecular characterization and is considered an excellent technique to investigate intra- and inter-molecular interactions.

In NMR spectroscopy, the magnetic shielding constant (σ) is an important parameter. When a nucleus is exposed to an external applied magnetic field (H_0) the electronic density will shield or deshield the atom. As a consequence, the nuclei experience an effective field such as

$$H_{eff} = (1-\sigma)H_0, \quad (1)$$

where σ is the nuclear magnetic shielding, which can assume either positive or negative values. For the first case ($\sigma>0$), $H_{eff} < H_0$, the nucleus is shielded. But in opposition, when $\sigma<0$ the nucleus is deshielded. Any effect that perturbs the electronic cloud changes σ that depends on the electronic density around the atom. The surrounding has particular importance on the NMR parameters because the environment can affect directly the molecular geometry and their electronic distribution. In particular, the solvent effect on NMR shielding constant can be splitted in different contributions: the bulk susceptibility, the anisotropy in the solvent susceptibility, the van der Waals interaction, the polar effect [3] and the hydrogen bond term. For this reason, there is a long discussion on the relative importance of these effects for a good theoretical description of magnetic shielding constants [4,5]. The shielding constant related to N, in particular, is of increasing interest for NMR characterization of organic compounds with biological importance [6–11]. In this context, the influence of the solute electronic polarization due to the solvent on the NMR parameters has been systematically discussed such as the spin-spin coupling [12] and the magnetic shielding constants [13–17].

In quantum mechanical simulations like Car-Parrinello or Born-Oppenheimer molecular dynamics the electronic polarization effects are naturally included. However, this is normally not the case for the usual force fields used in classical simulations such as Molecular Dynamics and Monte Carlo simulations. In this work we have used an iterative procedure that brings the solute electronic density in electrostatic equilibrium with the solvent [13,14,18]. This procedure is very efficient using instead of all configurations sampled just one average solvent electrostatic configuration (ASEC) [19] and will be better described

* Corresponding author.
E-mail address: vmanzoni@fis.ufal.br (V. Manzoni).

https://doi.org/10.1016/j.molliq.2020.114415
0167-7322/

below. This obtains the polarized atomic charges of the solute in the presence of the solvent. This iterative procedure was applied with success to describe several molecular properties, structural parameters [20], the electronic excitation spectra [13,14,21], nonlinear optical constants [22–25], as well as the NMR parameters of many chromophores [12,15–17,26]. Moreover, the solute-solvent hydrogen bond (H-bond) is another important tuning factor in NMR constants. For example, for aprotic nitrogen systems such as pyrimidine, experimental results indicate a cyclohexane-water experimental shift of 16.8 ppm on $\sigma(^{15}N)$ [27]. In other words, this means that the gas-solvent shift is positive ($\Delta\sigma>0$) and consequently the nitrogen nucleus is more shielded when the solvent is included, implying in an upfield effect [13,16]. On the other hand, some molecular compounds, such as ammonia, presents a contrast. In ammonia, the nitrogen arises under a pyramidal structure and performs H-bonds as a receptor (N···HX) or as a donor (NH···X) and contrary to azines, the environment decreases $\sigma(^{15}N)$ [12]. In fact, under gaseous conditions, experimental reports indicate a $\sigma(^{15}N)$ of 264.3 ppm for ammonia, which is changed to 241.7 ppm for liquid ammonia [12]. Therefore, if the isotope performs an H-bond donating the proton, the gas-solvent shift becomes negative ($\Delta\sigma<0$), decreasing $\sigma(^{15}N)$.

The general behavior of the ^{15}N shielding constants are not completely understood. For this reason, we started a series of studies on the main effects which enhance $\sigma(^{15}N)$ using explicit and implicit solvent models. These methodologies allow to include some of the most important interactions between solute and solvent. For this, the solvents were modelled classically by Monte Carlo simulation and the NMR properties were obtained by Quantum Mechanics. We have used the sequential Monte Carlo/Quantum Mechanics (s-MC/QM) methodology that first performs classical MC simulations generating statistically uncorrelated liquid structures composed by the solute and the solvent molecules for subsequent treatment with quantum mechanics [28–30]. The adopted methodology includes the solute polarization and uses several degrees of solvation including explicit solvent molecules in the quantum mechanics calculations. The main focus of this work is on the ^{15}N magnetic shielding of a protic chromophore. Therefore, besides revisiting some results for the NMR parameters of some previous nitrogen systems, we also discuss the solvent influence on the $\sigma(^{15}N)$ of hydrated formamide (FMA) (shown in Fig. 1). This molecule has particular importance for chemistry and biology because of its presence in peptide bonds, however, there are few information about its ^{15}N NMR parameters.

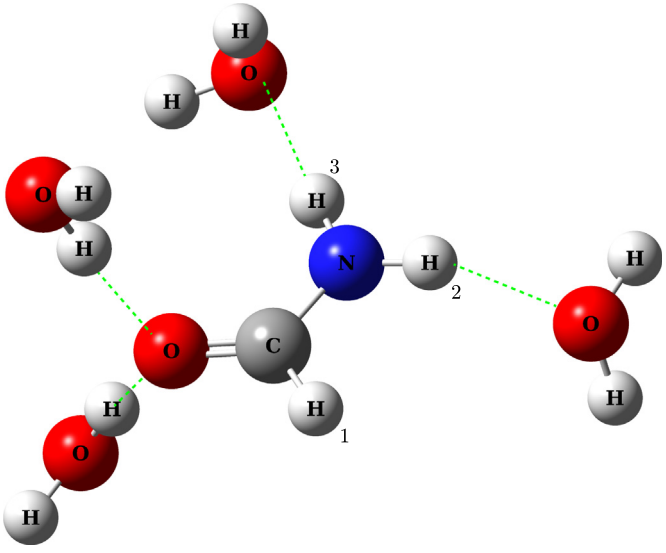

Fig. 1. A typical solute-solvent H-bond configuration of formamide sampled from the MC simulations. The green dashed line represent the hydrogen bonds.

2. Theory and computational details

The solvent effects on ^{15}N magnetic shielding constants of formamide were included using the s-MC/QM approach [30]. Hence, first classical MC simulations were performed to generate uncorrelated liquid structures and next QM calculations were performed on these supermolecular configurations. All classical Monte Carlo (MC) simulations were performed using the DICE code [31,32] using the *NpT* ensemble for one formamide molecule solvated by 1000 water molecules at 1.0 atm and 298 K. At this stage, all molecular interactions were modelled using the standard Lennard-Jones (LJ) plus Coulomb potential with the molecular geometry previously obtained at the MP2/aug-cc-pVQZ. The LJ parameters were obtained from the All-Atom Optimized Parameters For Liquid Simulation (AA-OPLS) [33]. The set of electronic charges implemented in the Coulomb potential was obtained using the CHarges from Electrostatic Potentials using a Grid-based method (CHELPG) [34]. The force field parameters used for the water molecules were obtained from the AA-OPLS.

The MC simulations were performed in two stages: (i) the thermalization process with 8×10^8 MC steps followed by (ii) the production stage with 7×10^9 MC steps. The polarization of the solute by the solvent was determined using the iterative procedure [13,14,18,35] that ensures the solute-solvent electrostatic equilibrium. This requires a series of simulations followed by QM calculations: After each iteration a new set of atomic charges for the solute was calculated using CHELPG and MP2/aug-cc-pVQZ calculation and using an average electrostatic configuration (ASEC) to represent the solvent, these new charges were adopted for the solute in a subsequent MC simulation. The procedure is iterated until the convergence within a predefined criterion. In fact we check on the of solute dipole moment.

The solvent effects on NMR properties were considered using four different solvent models:

1- **PCM:** The first is the Polarizable-Continuum Model within the Integral-Equation Formalism (IEF-PCM) [36,37]. This popular model of solvation describes the solvent as a continuum medium represented by its dielectric constant. This model requires great care when solute-solvent hydrogen-bonds are involved.
2- **ASEC:** After performing a classical MC simulation of the liquid, an Average Solvent Electrostatic Configuration [19] is generated from 200 uncorrelated MC structures composed by one solute surrounded by 500 water molecules considered as simple point charges at the atomic sites with the values corresponding to those obtained by CHELPG for FMA and AA-OPLS for water.
3- **HB:** QM calculations were performed on those configurations including the solvent molecules which are hydrogen-bonded to the solute. Therefore, 100 QM calculation were performed using uncorrelated configurations. At this level additional bulk water molecules are not considered.
4- **HBPC:** This complements the previous model adding to the hydrogen-bonded (HB) also the bulk solvent molecules treated as an electrostatic provided by 500 additional solvent water molecules considered as simple point charges. Therefore, the QM calculation were performed using 100 uncorrelated configurations composed of the solute formamide, the solute-solvent hydrogen bonded water molecules and in addition the outer solvent molecules treated as an simple point charges. This considers both the local HB specific interactions and the long-range electrostatic effects, becoming the best model used here.

All calculations were performed using the formamide gas phase geometry obtained by the second-order Møller-Plesset (MP2) methodology [38,39] with the aug-cc-pVQZ basis set [40–42]. The inclusion of the solvent effect in the geometry using PCM and the same MP2/aug-cc-pVQZ level gives only a mild change and is immaterial for the $\sigma(^{15}N)$ results. It changes the value from 173.1 ppm to 173.9 ppm and this justifies the use of gas phase geometry in our calculations. The ^{15}N

magnetic shielding constants were calculated using the Gauge-Independent Atomic Orbital (GIAO) method [43] with MP2 and density functional theory (DFT) based methods [44,45] with the 6-311++G(*d*, *p*) basis set [46]. All quantum mechanics calculations were performed using the Gaussian 09 package [47].

3. Results and discussions

The optimized geometric parameters are shown in Table 1. A very good agreement with experiment can be noted. The theoretical structure presents only small deviations in comparison with the experimental structure obtained with microwave spectroscopy [48]. For instance, *r*(CH_1), *r*(NH_2) and *r*(NH_3) are precisely obtained, and similar results are obtained for the angles.

3.1. The solute polarization and the liquid structure

The solute electronic polarization due to the solvent can be discussed by direct analysis of the molecular dipole moment (μ) of hydrated FMA. At this stage, all results for the isolated and solvated molecules were obtained at the MP2/aug-cc-pVQZ level.

The experimental estimated dipole moment for FMA in gas phase is 3.73 ± 0.07 D [49]. The MP2/aug-cc-pVQZ calculations obtained here is 3.88 D which is in good agreement with the experimental dipole moment. The solvent inclusion causes a polarization on FMA leading to an increasing dipole moment as observed in all solvation models considered. The simplest but very useful polarization scheme considered in this work is the continuum model (IEF-PCM). The calculations performed with this model gives the value of 4.92 D for hydrated FMA.

The more realistic polarization scheme was obtained using the iterative procedure starting from the gas phase charges obtained using CHELPG. After nine iteration steps the convergence was reached obtaining the dipole moment value of 6.32 D. This value corresponds to a solute polarization of 63% with respect to the gas phase values. This is the typical increasing of in-water polarization effects as previously obtained for solvated azines [13–16], ammonia [12] and uracil [17]. The convergence of the MP2 dipole moment calculated using the iterative procedures is shown in Fig. 2.

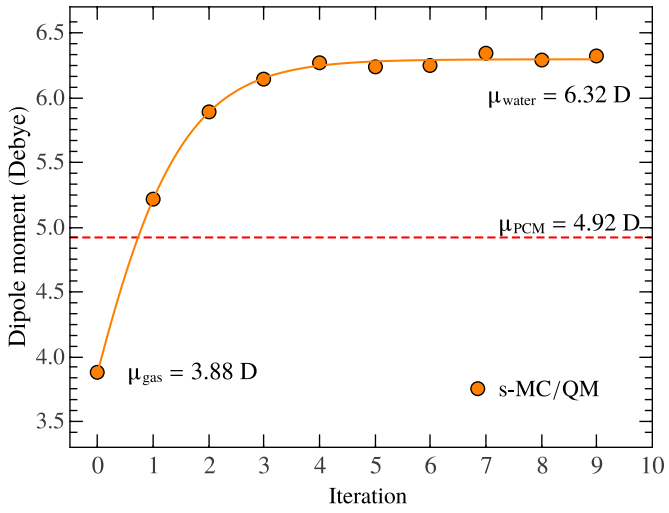

Fig. 2. The convergence of the dipole moment calculated with MP2/aug-cc-pVQZ in the iterative procedure.

3.2. Solute-solvent hydrogen bonds

The identification of the solute-solvent hydrogen bonds is very important for the characterization of the structure of the solvent around the solute molecule. This characterization is important because specifies the solvent molecules are treated explicitly in the subsequent QM calculations.

The formamide molecule has an acceptor of hydrogen bonds (CO group) and two donors (NH2 group). In our analysis, we pay attention to the solute-solvent hydrogen bonds formed in both the acceptor and donor groups of formamide. The statistical analysis of solute-solvent hydrogen bonds can be better performed using the combination of geometric and energetic criteria [13,14].

The geometric criterion can be established setting a cutoff distance between the solute acceptor or donor and the solvent donor or acceptor atoms respectively (r_{O-O} or r_{N-O}). This distance criterion was obtained by direct analysis of the radial distribution functions *G*(*r*) between the proton acceptor (or donor) atom of solute and the donor (or acceptor) atom of solvent showed in Fig. 3. The first peak maximum on $G(r)_{O-O}$ located at ~2.7 Å (*cf.* Fig. 3) suggests a larger number of solute-solvent hydrogen bonds.

The spherical integration of the first G(r) peak provide that the solvent can be bounded with an average of 2 hydrogen bonds with the NH2 proton donor group and 3 hydrogen bonds with the C═O proton acceptor group. The energetic criterion was established using a defined cutoff value in the pairwise energy distribution by direct analysis of the solute-solvent pairwise energy interaction histogram. For instance, the histogram of the pairwise energy interaction between formamide and water is shown in Fig. 4 for the better understanding of the energetic criteria. The distribution histogram of Fig. 4 shows the energy of the

Table 1
Theoretical and Experimental geometries for Formamide monomer. Bond lengths in angstroms and angles in degrees.

Parameter	Theoretical[a]	Experimental[b]	%
r(CN)	1.355	1.352	0.22
r(CO)	1.215	1.219	0.33
r(CH_1)	1.099	1.098	0.09
r(NH_2)	1.002	1.002	0.00
r(NH_3)	1.004	1.002	0.20
O—C—H_1	122.8	122.5	0.24
H_3—N—H_2	119.7	121.6	1.56
C—N—H_2	121.1	120.0	0.92
O—C—N	124.5	124.7	0.16

[a] Geometric parameter obtained at MP2/aug-cc-pVQZ level o quantum mechanics.
[b] Experimental parameters obtained with microwave spectroscopy [48].

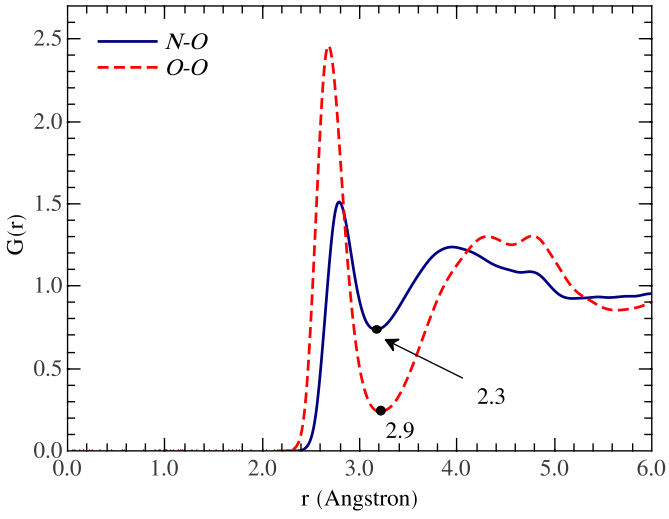

Fig. 3. Radial distribution functions between the nitrogen or oxygen atoms of formamide and the oxygen of water molecules. Also are shown the values obtained by spherical integration of first *G*(*r*) peaks.

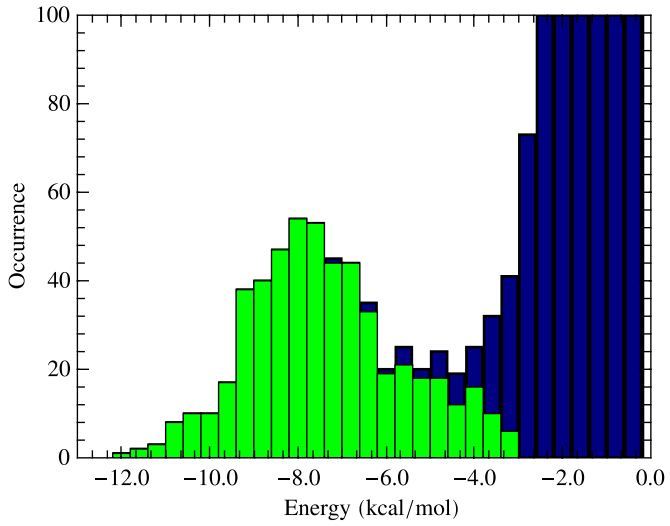

Fig. 4. Histogram of the pairwise energy interaction between formamide and water. In green (online) are shown the configurations selected with the HB criteria.

hydrogen bonds involved. We have thus selected the criterion of an energy below −3.0 kcal/mol. Using these analysis, the geometric and energetic criteria obtained were 3.2 Å for O—O and N—O distances and −3.0 kcal/mol for pairwise interaction energies. Also, the considered N-H-O and O-H-O angles cutoff were 45°.

The hydrogen bonded water molecules selected using these considered criteria can be visualized as function of their interaction energy with formamide and the corresponding distances using the diagram shown in Fig. 5. Using these defined criteria for the HB selection there are structures with two, three, four, five and six water molecules that make hydrogen bond with formamide. These structures were used for the ^{15}N NMR calculations and obey the following statistics: 1.6% of the configurations make two hydrogen bonds, 9.0% make three hydrogen bonds, 32.9% forms four hydrogen bonds, 54.3% make five hydrogen bonds and 2.2% forms six hydrogen bonds. Therefore, FMA forms an average of 4.5 hydrogen bonds with the surrounding water molecules.

3.3. ^{15}N magnetic shielding

The study of the solvent effects on the ^{15}N shielding constant is based on nonexplicit and explicit solvation models. The first group is represented by the Polarizable Continuum Model within the integral equation formalism variant (IEF-PCM). All considered explicit approximations are based on the configurations extracted from classical MC simulations. The ASEC is the first of them, and considers all explicit electrostatic interactions within the radial distance of 11 Å. The second explicit solvation model includes all solute-solvent HBs (HB model). The more realistic model considered in this work consider the solute-solvent HBs embedded in the electrostatic field of remaining 500 water molecules treated as simple point charges (HBPC). Besides the specific HB interactions, this model includes the long-range electrostatic interactions of the solvent bulk. The convergence of ^{15}N magnetic shielding calculations of FMA in explicit water (HBPC model) as function of the number of statistically uncorrelated configurations can be viewed in Fig. 6. All calculated ^{15}N magnetic shielding constants are performed using the MP2/6-311++G(*d*,*p*) and B97D/6-311++G(*d*,*p*) methods and these values are shown in Table 2.

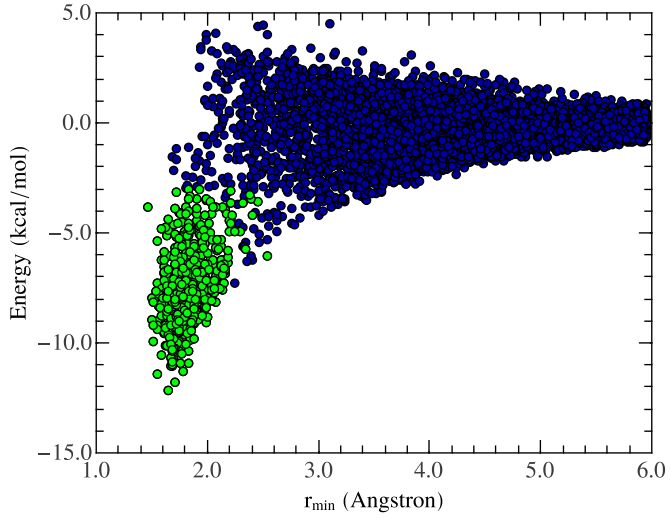

Fig. 5. Pairwise interaction energy between formamide and water. Also are showing the energy of water molecules hydrogen-bonded to formamide (in green).

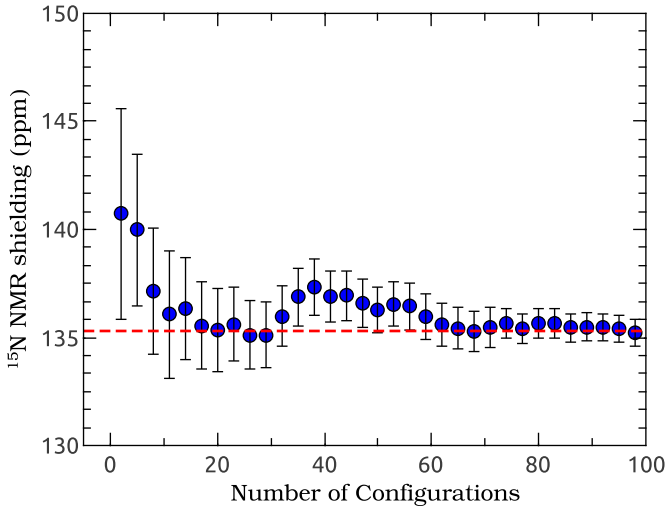

Fig. 6. Average $\sigma(^{15}N)$ calculated using MP2/6-311++G(*d*,*p*) method for FMA with the HBPC solvation model. The convergence using only HB is not shown because it presents a similar behavior.

The direct comparison between the ^{15}N shielding obtained using the MP2/6-311++G(*d*,*p*) and B97D/6-311++G(*d*,*p*) calculations shows that the DFT values are shifted by 24–26 ppm if compared with the values obtained using MP2/6-311++G(*d*,*p*). However, the calculated DFT gas-water ^{15}N NMR shielding shift ($\Delta\sigma$) are almost the same as obtained with MP2/6-311++G(*d*,*p*) for all solvent models considered. The calculated MP2/6-311++G(*d*,*p*) values of ^{15}N shielding constant for isolated FMA is 173.1 ppm, which is in reasonable accordance with the theoretical value of 167.7 ppm estimated by Vaara et al. [48]. The direct comparison of theoretical and experimental values in water of ^{15}N shielding constants is difficult due to the scarcity of ^{15}N NMR results for FMA in solvent environment. However, Vaara and co-workers also obtained the $\sigma(^{15}N)$ for FMA in the liquid phase as 152.5 ppm [48].

Table 2
The ^{15}N magnetic shielding constants (σ/ppm), and the gas to solvent shift ($\Delta\sigma$/ppm) calculated using the MP2/6-311++G(*d*,*p*) and B97D/6-311++G(*d*,*p*) methodologies.

		Gas	PCM	ASEC	HB	HBPC	Experimental
MP2	σ	173.1	163.9	150.0	146.0 ± 0.7	135.2 ± 0.7	152.5[a]
	$\Delta\sigma$		−9.2	−23.1	−27.1 ±0.7	−37.9 ± 0.7	−15.2[b]
B97D	σ	148.6	137.9	125.3	121.3 ± 0.7	110.1 ± 0.8	152.5[a]
	$\Delta\sigma$		−9.6	−23.3	−27.3 ±0.7	−38.5 ± 0.8	−15.2[b]

[a] The experimental results were measured for the liquid FMA [48].
[b] Value obtained considering as reference the estimation of 167.7 ppm calculated with the experimental microwave geometry [48]. Uncertainty shown are statistical errors.

Using this value Vaara could estimate a gas-solvent shift of −15.2 ppm. This result is in line with our previous finding [13,14,16] that the shifts follow much better the Reichardt solvent polarity scale [50] than the simplistic trend of the dielectric constant. In the Reichardt scale the formamide and water have polarities 0.775 and 1.000 respectively, It is thus expected that the absolute values of the formamide ^{15}N NMR gas-water shifts should be larger than gas-liquid shift. Also, performing a direct comparison between the formamide and water polarities together with the gas-liquid obtained by Vaara one can estimate that the gas-water shift must be negative and with absolute values larger than 15.2 ppm.

The IEF-PCM calculation predicts a ^{15}N shielding constant of 163.9 ppm, meaning a downfield of −9.2 ppm compared to the calculated gas phase value. Therefore, this result indicates that the continuum model is not able to provide the correct order of magnitude of the ^{15}N NMR gas-water shifts of FMA.

The iterative polarization provides a decrease in the ^{15}N shielding constant if compared with gas phase for all models of solvent considered. The calculations using ASEC give a shielding constant of 150.0 ppm, which implies in a gas-solvent shift of −23.1 ppm. The HB model, which includes all solvent molecules bounded to Formamide by H-bond interactions (see Fig. 1) does not improve the prediction but confirms its trend. The HB solvent model indicates a shielding constant of 146.0 ± 0.7 ppm. Therefore, the solvent inclusion as HB induces a deshielding around of 27 ppm. This value shows the contribution of the hydrogen bonds on the ^{15}N NMR shielding constant of FMA.

Significant informations are obtained when the HBPC model is considered for modelling the solvent. This model includes the specific hydrogen bond interactions obtained by MC simulations together with the long-range electrostatic contributions from the remaining bulk molecules. This approximation provides the value of 135.2 ± 0.7 ppm. This value indicates a strong deshielding effects of 37.9 ± 0.7 ppm after the water inclusion. As consequence, $\Delta\sigma(^{15}N)<0$ and these calculated absolute values are larger than 15.2 ppm obtained for liquid FMA by Vaara et al. [48], as expected.

The total NMR shielding may be split as a sum of a diamagnetic (σ_d) and paramagnetic (σ_p) contributions. The diamagnetic term is the shielding caused by the spherical part of the electronic density distribution and the paramagnetic term is associated to $p(l=1)$ or higher angular momentum that provides a nonspherical electronic density around the nucleus. A detailed analysis of diamagnetic and paramagnetic terms requires the complicated analysis of the wave function besides the knowledge of the excited electronic states of the molecule [51]. However, here we are only focusing on analyzing the contribution of diamagnetic and paramagnetic parts of ^{15}N NMR shielding constant of FMA. In this context, in Table 3 are shown the B97D/6-311++G(*d*,*p*) values obtained for the diamagnetic and paramagnetic contributions to the ^{15}N NMR shielding constant of FMA in gas phase and in water considering several solvent models.

Under gaseous conditions the diamagnetic ^{15}N NMR shielding constant σ_d is calculated as 322.2 ppm, and it remains almost unaltered when the system is hydrated in all models of solvent considered. However, the σ_p presents different behavior. For the isolated FMA, the paramagnetic term is −175.1 ppm. But in aqueous environment, the IEF-PCM formalism points to a lower contribution of −183.9 ppm. The use of the simple electrostatic approximation (ASEC) gives a paramagnetic ^{15}N NMR shielding of −197.5 ppm. Including only the hydrogen bonded water molecules (HB model) the paramagnetic ^{15}N NMR shielding is −203.0 ± 0.8. The inclusion of the hydrogen bonded water molecules plus the electrostatic bulk (HBPC model) provides the value of −214.0 ± 0.8 for the paramagnetic part of ^{15}N NMR shielding of FMA. Furthermore, the paramagnetic contribution is the main responsible for the gas-solvent shift of the ^{15}N NMR shielding of solvated formamide.

We now compare our results with some other nitrogenous systems in an attempt to understand the general behavior of the solvent effect on ^{15}N NMR shielding constants. The solvent effect on ^{15}N NMR shielding constant depends on the hydrogen bond donor or acceptor capacity of the reference nitrogen atom of the solute surrounded by the solvent environment. For instance, the nitrogen atoms of azines molecules only can form N···HX H-bonds (acceptor of HB). Particularly, a positive gas-water shift of azines were reported by several works [13–16,52,53] and these shifts are shown in Table 4. These values range from 14.9 ppm to 38.9 ppm. [13]. These systems have been systematically reviewed and all results indicate that both the continuous and explicit models can give the correct trend of the solvent shift. Furthermore, the results obtained for models that include explicitly the hydrogen bonded solvent molecules plus the electrostatic bulk are similar to the results obtained only with the electrostatic interactions of the bulk providing a good concordance with experimental results as can be seen in references [13–16]. These results are in contrast with the results obtained here for FMA: (i) the FMA has a negative gas-solvent shift and (ii) the electrostatic model (ASEC) is able to provide only around of 60% of the total gas-water shift if compared with the HBPC model; (iii) only including hydrogen bonded molecules supply only 71% of the total gas-water shift if compared with HBPC results (see Table 2). This result indicates the large influence of explicit hydrogen bonds and the need for inclusion of the electrostatic bulk effect for a good description of gas-water shift of FMA.

The general behavior of ^{15}N NMR shielding of FMA in water is very similar to the behavior presented for liquid ammonia, in which the nitrogen atom also performs H-bond like NH···X. In ammonia, experimental results report ^{15}N shielding constant of 264.3 ppm for isolated molecule and in liquid environment this quantity decreases to 241.7 ppm [54]. However, the liquid phase of ammonia causes a deshield of 22.6 ppm if compared with gas phase. More sophisticated theoretical approach which includes different levels of including the effects of the solvent such as the solute polarization due to environment and effects of geometrical relaxation confirms a negative gas-solvent shift of −25.2 ± 1.0 ppm for ammonia after the inclusion of some explicit solute-solvent hydrogen bonded molecules plus the electrostatic effect of the solvent [12]. However, the inclusion of the solvent represented only by electrostatic interaction in liquid ammonia (ASEC

Table 3
Diamagnetic (σ_d/ppm) and paramagnetic (σ_p/ppm) contributions of ^{15}N NMR shielding of FMA calculated at the B97D/6-311++G(*d*,*p*) level.

	Gas	ASEC	PCM	HB	HBPC
σ_d	322.2	322.5	321.5	324.0 ± 0.2	323.5 ± 0.2
$\Delta\sigma_d$		0.3	−0.7	1.8 ± 0.2	1.3 ± 0.2
σ_p	−175.1	−197.5	−183.9	−203.0 ± 0.7	−214.0 ± 0.8
$\Delta\sigma_p$		−22.4	−8.8	−27.9 ± 0.7	−38.9 ± 0.8
Total[a]	147.1	125.1	137.7	120.9 ± 0.7	109.5 ± 0.8
Shift		−22.0	−9.4	−26.2 ± 0.7	−37.6 ± 0.8

[a] The σ_p and σ_d are calculated using only the contributions of the most relevant orbitals. For this reason, $\sigma_p + \sigma_d$ is slightly different from σ total.

Table 4
Experimental (extracted from the references) and theoretical results for σ (ppm) and $\Delta\sigma$ (ppm) obtained for some nitrogen systems.

H-bond	System	σ_{gas}	$\sigma_{solvent}$	$\Delta\sigma$	Ref.
NH···X	Ammonia	259.9	234.7	−25.2	[12][a]
		264.3	241.7	−22.6	[54][b]
N···HX	Pyridine	−111.4	−72.5	38.9	[16][a]
		−110.2	−61.8	50.3	[15][a]
		−102.8	−82.5	20.3	[52][a]
		−84.4	−56.3	28.1	[53][b]
N···HX	1,2-Diazine	−229.6	−184.6	45.0	[16][a]
	1,3-Diazine	−83.7	−61.3	22.4	[16][a]
	1,4-Diazine	−127.0	−110.2	16.8	[16][a]
	1,3,5-Triazine	−65.4	−50.5	14.9	[16][a]

[a] Theoretical value.
[b] Experimental value.

model) gives a wrong behavior of the gas-liquid shift [12] in contrast with the correct tendency obtained here for FMA using the ASEC method (*cf.* Table 2). However, despite that both liquid ammonia and in-water FMA can make H-bonds like NH···X in the case of liquid ammonia H-bonds like N···HX can also be found. Therefore, the incomplete description of the solvent due the lack of specific interactions such as hydrogen bonds in the Nitrogen atom is the main cause for the wrong behavior of gas-liquid shift of ammonia using the ASEC model. This is because the lone pair electrons play a very important role in determining the magnitude of the paramagnetic component of ^{15}N NMR shielding constant as shown previously [55].

4. Conclusions

In this work we present a detailed study of the solvent effects on the ^{15}N magnetic shielding of formamide in water using different solvent models. Both implicit and explicit models of solvent were employed. For the explicit models considered the solvent is included using Monte Carlo in the s-MC/QM approach. In this methodology first a classical MC simulations was performed to generate uncorrelated liquid structures and next QM calculations were performed using the generated supermolecular solute-solvent configurations to obtain the statistically converged ^{15}N magnetic shielding constant of FMA. The presence of the solvent causes an intramolecular redistribution of the electronic charges of the solute, which alters the properties of interest. The dipole moment, for instance, increases 63% compared to its value calculated for isolated FMA. The solvent effect was included using a methodology that can be used to estimate individually the following solvent contributions: (i) the electrostatic interactions; (ii) only the solvent hydrogen bonds; (iii) the combination between the hydrogen bonds and the electrostatic bulk. This methodology allowed to comprehend the solvent effects that enhance $\sigma(^{15}N)$. The results indicate that consideration of the solute polarization due to the environment is important to understand the NMR shielding. It is shown that the paramagnetic contribution to the magnetic shielding is more sensitive for the environment being largely responsible to the total gas-water calculated shift. In summary, our results show that all considered explicit and implicit solvent models provide the correct deshielding tendency of the gas-water ^{15}N NMR shift of FMA. Also the models that lack inclusion of explicit solvent hydrogen bonds underestimate the total gas-water ^{15}N NMR shift of FMA. Therefore, all results point to the large influence of hydrogen bonds on ^{15}N NMR shielding constants of FMA and suggest the need to include it and complement with the electrostatic effect of the outer solvent molecules to obtain a good description of gas-water shift of FMA. The direct comparison between other nitrogen systems indicate that hydrogen bonds where the solute is the proton donor is relevant for the ^{15}N NMR shielding calculation.

CRediT authorship contribution statement

Rodrigo Gester: Methodology, Software, Investigation, Writing - original draft. **Marcus V.A. Damasceno:** Software, Investigation, Data curation. **Sylvio Canuto:** Methodology, Investigation, Writing - review & editing. **Vinícius Manzoni:** Conceptualization, Methodology, Investigation, Writing - review & editing, Supervision.

Declaration of competing interest

The authors declare that they have no known competing financial interests or personal relationships that could have appeared to influence the work reported in this paper.

Acknowledgments

The authors are grateful to Brazilian funding agencies Fundação de Amparo à Pesquisa do Estado de Alagoas (FAPEAL), Coordenação de Aperfeiçoamento de Pessoal de Ensino Superior (CAPES), Conselho Nacional de Desenvolvimento Científico e Tecnológico (CNPq) and Fundação de Amparo à Pesquisa do Estado de São Paulo (FAPESP).

References

[1] F. Castellani, B. van Rossum, A. Diehl, M. Schubert, K. Rehbein, H. Oschkinat, Structure of a protein determined by solid-state magic-angle-spinning NMR spectroscopy, Nature 420 (6911) (2002) 99–102, https://doi.org/10.1038/nature01070.
[2] A. Loquet, B. Bardiaux, C. Gardiennet, C. Blanchet, M. Baldus, M. Nilges, T. Malliavin, A. Böckmann, 3d structure determination of the Crh protein from highly ambiguous solid-state NMR restraints, J. Am. Chem. Soc. 130 (11) (2008) 3579–3589, https://doi.org/10.1021/ja078014t.
[3] A.D. Buckingham, T. Schaefer, W.G. Schneider, Solvent effects in nuclear magnetic resonance spectra, J. Chem. Phys. 32 (4) (1960) 1227–1233, https://doi.org/10.1063/1.1730879.
[4] C.J. Jameson, Gas-phase NMR spectroscopy, Chem. Rev. 91 (7) (1991) 1375–1395, https://doi.org/10.1021/cr00007a005.
[5] T. Helgaker, M. Jaszuński, K. Ruud, Ab initio methods for the calculation of NMR shielding and indirect spin-spin coupling constants, Chem. Rev. 99 (1) (1999) 293–352, https://doi.org/10.1021/cr960017t.
[6] J. Mason, Nitrogen nuclear magnetic resonance spectroscopy in inorganic, organometallic, and bioinorganic chemistry, Chem. Rev. 81 (3) (1981) 205–227, https://doi.org/10.1021/cr00043a001.
[7] C.J. Markin, L.F. Saltibus, L. Spyracopoulos, Dynamics of the ring domain from human TRAF6 by 15N NMR spectroscopy: implications for biological function, Biochemistry 47 (38) (2008) 10010–10017, https://doi.org/10.1021/bi800252x.
[8] L. Banci, I. Bertini, C. Cavazza, I.C. Felli, D. Koulougliotis, Probing the backbone dynamics of oxidized and reduced rat microsomal cytochrome b5 via 15N rotating frame NMR relaxation measurements: biological implications, Biochemistry 37 (35) (1998) 12320–12330, https://doi.org/10.1021/bi980885f.
[9] C.D. Kroenke, J.P. Loria, L.K. Lee, M. Rance, A.G. Palmer, Longitudinal and transverse 1H-15N dipolar/15n chemical shift anisotropy relaxation interference: unambiguous determination of rotational diffusion tensors and chemical exchange effects in biological macromolecules, J. Am. Chem. Soc. 120 (31) (1998) 7905–7915, https://doi.org/10.1021/ja980832l.
[10] E.N.G. Marsh, Y. Suzuki, Using 19F NMR to probe biological interactions of proteins and peptides, ACS Chem. Biol. 9 (6) (2014) 1242–1250, https://doi.org/10.1021/cb500111u.
[11] V.H. Pomin, J.S. Sharp, X. Li, L. Wang, J.H. Prestegard, Characterization of glycosaminoglycans by 15N NMR spectroscopy and in vivo isotopic labeling, Anal. Chem. 82 (10) (2010) 4078–4088, https://doi.org/10.1021/ac1001383.
[12] R.M. Gester, H.C. Georg, S. Canuto, M.C. Caputo, P.F. Provasi, NMR chemical shielding and spin-spin coupling constants of liquid NH3: a systematic investigation using the sequential QM/MM method, J. Phys. Chem. A 113 (52) (2009) 14936–14942, https://doi.org/10.1021/jp9050484.
[13] V. Manzoni, M.L. Lyra, R.M. Gester, K. Coutinho, S. Canuto, Study of the optical and magnetic properties of pyrimidine in water combining PCM and QM/MM methodologies, Phys. Chem. Chem. Phys. 12 (42) (2010), 14023, https://doi.org/10.1039/c0cp00122h.
[14] V. Manzoni, M.L. Lyra, K. Coutinho, S. Canuto, Comparison of polarizable continuum model and quantum mechanics/molecular mechanics solute electronic polarization: study of the optical and magnetic properties of diazines in water, J. Chem. Phys. 135 (14) (2011), 144103, https://doi.org/10.1063/1.3644894.
[15] R.M. Gester, H.C. Georg, T.L. Fonseca, P.F. Provasi, S. Canuto, A simple analysis of the influence of the solvent-induced electronic polarization on the 15N magnetic shielding of pyridine in water, Theor. Chem. Accounts 131 (5) (2012) 1220, https://doi.org/10.1007/s00214-012-1220-0.
[16] L. Modesto-Costa, R.M. Gester, V. Manzoni, The role of electrostatic interactions and solvent polarity on the 15N NMR shielding of azines, Chem. Phys. Lett. 686 (2017) 189–194, https://doi.org/10.1016/j.cplett.2017.08.031.
[17] R.M. Gester, C. Bistafa, H.C. Georg, K. Coutinho, S. Canuto, Theoretically describing the 17O magnetic shielding constant of biomolecular systems: uracil and 5-fluorouracil in water environment, Theor. Chem. Accounts 133 (1) (2013) 1424, https://doi.org/10.1007/s00214-013-1424-y.
[18] H.C. Georg, K. Coutinho, S. Canuto, Solvent effects on the uv-visible absorption spectrum of benzophenone in water: a combined Monte Carlo quantum mechanics study including solute polarization, J. Chem. Phys. 126 (3) (2007), 034507, https://doi.org/10.1063/1.2426346.
[19] K. Coutinho, H. Georg, T. Fonseca, V. Ludwig, S. Canuto, An efficient statistically converged average configuration for solvent effects, Chem. Phys. Lett. 437 (1–3) (2007) 148–152, https://doi.org/10.1016/j.cplett.2007.02.012.
[20] L.R. Franco, I. Brandão, T.L. Fonseca, H.C. Georg, Elucidating the structure of merocyanine dyes with the ASEC-FEG method. Phenol blue in solution, J. Chem. Phys. 145 (19) (2016), 194301, https://doi.org/10.1063/1.4967290.
[21] C. Bistafa, H.C. Georg, S. Canuto, Combining ab initio multiconfigurational and free energy gradient methods to study the pi-pi* excited state structure and properties of uracil in water, Computational and Theoretical Chemistry 1040-1041 (2014) 312–320, https://doi.org/10.1016/j.comptc.2014.04.024.
[22] O. Santos, J. Sabino, H. Georg, T. Fonseca, M. Castro, Electric properties of the 3-methyl-4-nitropyridine-1-oxyde (POM) molecules in solid phase: a theoretical study including environment polarization effect, Chem. Phys. Lett. 669 (2017) 176–180, https://doi.org/10.1016/j.cplett.2016.12.042.
[23] V. Manzoni, L. Modesto-Costa, J.D. Nero, T. Andrade-Filho, R. Gester, Strong enhancement of NLO response of methyl orange dyes through solvent effects: a sequential

Monte Carlo/DFT investigation, Opt. Mater. 94 (2019) 152–159, https://doi.org/10.1016/j.optmat.2019.05.018.
[24] J. Quertinmont, B. Champagne, F. Castet, M.H. Cardenuto, Explicit versus implicit solvation effects on the first hyperpolarizability of an organic biphotochrome, J. Phys. Chem. A 119 (21) (2015) 5496–5503, https://doi.org/10.1021/acs.jpca.5b00631.
[25] M.H. Cardenuto, F. Castet, B. Champagne, Investigating the first hyperpolarizability of liquid carbon tetrachloride, RSC Adv. 6 (101) (2016) 99558–99563, https://doi.org/10.1039/c6ra23187j.
[26] M.C. Caputo, P.F. Provasi, L. Benitez, H.C. Georg, S. Canuto, K. Coutinho, Monte carlo–quantum mechanics study of magnetic properties of hydrogen peroxide in liquid water, J. Phys. Chem. A 118 (32) (2014) 6239–6247, https://doi.org/10.1021/jp411303n.
[27] M. Witanowski, W. Sicinska, S. Biernat, G. Webb, Solvent effects on nitrogen NMR shieldings in azines, J. Magn. Reson. 91 (2) (1991) 289–300, https://doi.org/10.1016/0022-2364(91)90193-W.
[28] W.R. Rocha, V.M. Martins, K. Coutinho, S. Canuto, Solvent effects on the electronic absorption spectrum of formamide studied by a sequential Monte Carlo/quantum mechanical approach, Theor. Chem. Accounts 108 (1) (2002) 31–37, https://doi.org/10.1007/s00214-002-0353-y.
[29] W.R. Rocha, K. Coutinho, W.B. de Almeida, S. Canuto, An efficient quantum mechanical/molecular mechanics Monte Carlo simulation of liquid water, Chem. Phys. Lett. 335 (1) (2001) 127–133, https://doi.org/10.1016/S0009-2614(01)00024-0.
[30] K. Coutinho, S. Canuto, Solvent effects in emission spectroscopy: a Monte Carlo quantum mechanics study of the n<-pi* shift of formaldehyde in water, J. Chem. Phys. 113 (20) (2000) 9132–9139, https://doi.org/10.1063/1.1320827.
[31] K. Coutinho, S. Canuto, Dice: A Monte Carlo Program for Molecular Liquid Simulation, 2003.
[32] H.M. Cezar, S. Canuto, K. Coutinho, Dice: a Monte Carlo code for molecular simulation including configurational bias Monte Carlo method, J. Chem. Inf. Model. 60 (7) (2020) 3472–3488, https://doi.org/10.1021/acs.jcim.0c00077.
[33] J. Pranata, S.G. Wierschke, W.L. Jorgensen, Opls potential functions for nucleotide bases. Relative association constants of hydrogen-bonded base pairs in chloroform, J. Am. Chem. Soc. 113 (8) (1991) 2810–2819, https://doi.org/10.1021/ja00008a002.
[34] C.M. Breneman, K.B. Wiberg, Determining atom-centered monopoles from molecular electrostatic potentials. The need for high sampling density in formamide conformational analysis, J. Comput. Chem. 11 (3) (1990) 361–373, https://doi.org/10.1002/jcc.540110311.
[35] R.C. Barreto, K. Coutinho, H.C. Georg, S. Canuto, Combined Monte Carlo and quantum mechanics study of the solvatochromism of phenol in water. The origin of the blue shift of the lowest pi-pi* transition, Phys. Chem. Chem. Phys. 11 (2009) 1388–1396, https://doi.org/10.1039/B816912H.
[36] J. Tomasi, B. Mennucci, E. Cances, The IEF version of the PCM solvation method: an overview of a new method addressed to study molecular solutes at the QM ab initio level, J. Mol. Struct. THEOCHEM 464 (1) (1999) 211–226, https://doi.org/10.1016/S0166-1280(98)00553-3.
[37] J. Tomasi, B. Mennucci, R. Cammi, Quantum mechanical continuum solvation models, Chem. Rev. 105 (8) (2005) 2999–3094, https://doi.org/10.1021/cr9904009.
[38] C. Møller, M.S. Plesset, Note on an approximation treatment for many-electron systems, Phys. Rev. 46 (1934) 618, https://doi.org/10.1103/PhysRev.46.618.
[39] M.J. Frisch, M. Head-Gordon, J.A. Pople, A direct MP2 gradient method, Chem. Phys. Lett. 166 (1990) 275, https://doi.org/10.1016/0009-2614(90)80029-D.
[40] R.A. Kendall, T.H. Dunning, R.J. Harrison, Electron affinities of the first-row atoms revisited. Systematic basis sets and wave functions, J. Chem. Phys. 96 (9) (1992) 6796–6806, https://doi.org/10.1063/1.462569.
[41] D.E. Woon, T.H. Dunning, Gaussian basis sets for use in correlated molecular calculations. III. The atoms aluminum through argon, J. Chem. Phys. 98 (2) (1993) 1358–1371, https://doi.org/10.1063/1.464303.
[42] T.H. Dunning, Gaussian basis sets for use in correlated molecular calculations. i. the atoms boron through neon and hydrogen, J. Chem. Phys. 90 (2) (1989) 1007–1023, https://doi.org/10.1063/1.456153.
[43] K. Wolinski, J.F. Hinton, P. Pulay, Efficient implementation of the gauge-independent atomic orbital method for NMR chemical shift calculations, J. Am. Chem. Soc. 112 (23) (1990) 8251–8260, https://doi.org/10.1021/ja00179a005.
[44] P. Hohenberg, W. Kohn, Inhomogeneous electron gas, Phys. Rev. 136 (1964) B864, https://doi.org/10.1103/PhysRev.136.B864.
[45] W. Kohn, L.J. Sham, Self-consistent equations including exchange and correlation effects, Phys. Rev. 140 (1965) A1133, https://doi.org/10.1103/PhysRev.140.A1133.
[46] R. Krishnan, J.S. Binkley, R. Seeger, J.A. Pople, Self-consistent molecular orbital methods. XX. A basis set for correlated wave functions, J. Chem. Phys. 72 (1) (1980) 650–654, https://doi.org/10.1063/1.438955.
[47] M.J. Frisch, G.W. Trucks, H.B. Schlegel, G.E. Scuseria, M.A. Robb, J.R. Cheeseman, G. Scalmani, V. Barone, B. Mennucci, G.A. Petersson, H. Nakatsuji, M. Caricato, X. Li, H.P. Hratchian, A.F. Izmaylov, J. Bloino, G. Zheng, J.L. Sonnenberg, M. Hada, M. Ehara, K. Toyota, R. Fukuda, J. Hasegawa, M. Ishida, T. Nakajima, Y. Honda, O. Kitao, H. Nakai, T. Vreven, J.A. Montgomery Jr., J.E. Peralta, F. Ogliaro, M. Bearpark, J.J. Heyd, E. Brothers, K.N. Kudin, V.N. Staroverov, T. Keith, R. Kobayashi, J. Normand, K. Raghavachari, A. Rendell, J.C. Burant, S.S. Iyengar, J. Tomasi, M. Cossi, N. Rega, J.M. Millam, M. Klene, J.E. Knox, J.B. Cross, V. Bakken, C. Adamo, J. Jaramillo, R. Gomperts, R.E. Stratmann, O. Yazyev, A.J. Austin, R. Cammi, C. Pomelli, J.W. Ochterski, R.L. Martin, K. Morokuma, V.G. Zakrzewski, G.A. Voth, P. Salvador, J.J. Dannenberg, S. Dapprich, A.D. Daniels, O. Farkas, J.B. Foresman, J.V. Ortiz, J. Cioslowski, D.J. Fox, Gaussian 09 Revision C.01, 2010.
[48] J. Vaara, J. Kaski, J. Jokisaari, P. Diehl, NMR properties of formamide: a first principles and experimental study, J. Phys. Chem. A 101 (28) (1997) 5069–5081, https://doi.org/10.1021/jp970287v.
[49] D.W. Rankin, CRC Handbook of Chemistry and Physics, 89th edition, edited by David R. Lide, Crystallogr. Rev. 15 (3) (2009) 223–224, https://doi.org/10.1080/08893110902764125.
[50] C. Reichardt, Solvatochromic dyes as solvent polarity indicators, Chem. Rev. 94 (8) (1994) 2319–2358, https://doi.org/10.1021/cr00032a005.
[51] P. Pyykkö, Perspective on Norman Ramsey's theories of NMR chemical shifts and nuclear spin–spin coupling, Theor. Chem. Accounts 103 (3) (2000) 214–216, https://doi.org/10.1007/s002149900011.
[52] B. Mennucci, J.M. Martínez, J. Tomasi, Solvent effects on nuclear shieldings: continuum or discrete solvation models to treat hydrogen bond and polarity effects? J. Phys. Chem. A 105 (30) (2001) 7287–7296, https://doi.org/10.1021/jp010837w.
[53] R.O. Duthaler, J.D. Roberts, Effects of solvent, protonation, and n-alkylation on the nitrogen-15 chemical shifts of pyridine and related compounds, J. Am. Chem. Soc. 100 (16) (1978) 4969–4973, https://doi.org/10.1021/ja00484a008.
[54] M. Alei, A.E. Florin, W.M. Litchman, J.F. O'Brien, Nitrogen-15 nuclear magnetic resonance shifts in pure methylamines and pure methyl isocyanide-nitrogen-15, J. Phys. Chem. 75 (7) (1971) 932–938, https://doi.org/10.1021/j100677a016.
[55] G.A. Webb, M. Witanowski, Nitrogen NMR and molecular interations, Proceedings of the Indian Academy of Sciences-Chemical Sciences 94 (2) (1985) 241–290, https://doi.org/10.1007/BF02860225.